THE JOURNAL OF BIOLOGICAL CHEMISTRY
Vol. 279, No. 22, Issue of May 28, pp. 23790–23796, 2004
Printed in U.S.A.

Distribution and Transport of Cholesterol-rich Membrane Domains Monitored by a Membrane-impermeant Fluorescent Polyethylene Glycol-derivatized Cholesterol*

Received for publication, December 11, 2003, and in revised form, March 5, 2004
Published, JBC Papers in Press, March 16, 2004, DOI 10.1074/jbc.M313568200

Satoshi B. Sato‡§¶, Kumiko Ishii‡, Asami Makino‡, Kazuhisa Iwabuchi‡‖, Akiko Yamaji-Hasegawa‡, Yukiko Senoh‡, Isao Nagaoka‖, Hitoshi Sakuraba‡‡, and Toshihide Kobayashi‡§§¶¶**

From the ‡RIKEN, Wako, Saitama 351-0198, Japan, §Department of Biophysics, Graduate School of Science, Kyoto University, Kyoto 606-8502, Japan, ‖Department of Biochemistry, Juntendo University, School of Medicine, Bunkyo-ku, Tokyo 113-8421, Japan, ‡‡Department of Clinical Genetics, The Tokyo Metropolitan Organization of Medical Research, Bunkyo-ku, Tokyo 113-8613, Japan, and §§INSERM U585, Institut National des Sciences Appliquees-Lyon, 69621 Villeurbanne, France

Cholesterol-rich membrane domains function in various membrane events as diverse as signal transduction and membrane traffic. We studied the interaction of a fluorescein ester of polyethylene glycol-derivatized cholesterol (fPEG-Chol) with cholesterol-rich membranes both in cells and in model membranes. Unlike filipin and other cholesterol probes, this molecule could be applied as an aqueous dispersion to various samples. When added to live cells, fPEG-Chol distributed exclusively in the outer plasma membrane leaflet and was enriched in microdomains that dynamically clustered by the activation of receptor signaling. The surface-bound fPEG-Chol was slowly internalized via clathrin-independent pathway into endosomes together with lipid raft markers. Noteworthy, fPEG-Chol could be microinjected in the living cells in which we found Golgi apparatus as the sole major organelle to be labeled. PEG-Chol, thus, provides a novel, sensitive probe for unraveling the dynamics of cholesterol-rich microdomains in living cells.

The content and distribution of cholesterol is regulated dynamically by complex mechanisms. Inside the mammalian cells a graded level of free cholesterol distributes in various membrane organelles, with the highest accumulation as domains in the post-Golgi membranes (1). In the plasma membrane cholesterol is also accumulated in microdomains with specific phospholipids such as sphingomyelin. These domains, often referred to lipid rafts, ubiquitously distribute from yeast to mammals, playing important roles in cellular functions (2–5). Removal of cell surface cholesterol by methyl-β-cyclodextrin (MβCD)[1] results in disintegration of these domains, affecting diverse activities such as signaling, adhesion, motility, and membrane trafficking (6, 7).

Little is known, however, about the membrane trafficking of cholesterol in live cells. This is apparently due to the lack of sensitive probes. In addition to the specificity as a precondition, use of a small amount of highly sensitive probe is necessary since probing the dynamics relies on the lowest impact of the function of the cholesterol-containing domains. Moreover, cholesterol is very unique in that its level in various membranes is tightly linked even to the transcriptional or secretory activity (8). Therefore, when using a small molecule as a probe, its insertion at a high numbered residue in functioning membranes should be avoided to reduce unexpected impact on the cellular activities. In this respect, filipin, which can be successfully used to detect cholesterol in fixed cells, is not suitable for live cells studies since, in addition to the poor fluorescence property, it yields a cytotoxic side effect by sequestering cholesterol. Similarly, using cholesterol-binding proteins as probes, which accumulate cholesterol and even form pores, often becomes problematic.

Polyethylene glycol cholesteryl ethers (PEG-Chols) are a unique group of non-ionic amphiphatic cholesterol derivatives (Fig. 1) (9). Because of low toxicity, various PEG-Chols were initially used *in vivo* to disperse otherwise water-insoluble antibiotics (10). Recently it was reported that PEG(50)-Chol ($M_r \sim 2600$; 50 is average number of PEG repeats) was singly dispersed in aqueous media and distributed on the surface of cultured cells (9, 11). Without affecting the clathrin-dependent endocytosis, PEG(50)-Chol could inhibit caveolae-like endocytosis in A431 cells, although the required amount was as high as 3×10^8 molecules/cell (11). This specificity suggests that PEG-Chols may interact with specific membrane components at much lower dose.

In the present study we showed that a fluorescein-tagged

* This work was supported by grants from RIKEN Frontier Research System (to T. K.), Bioarchitect Research Project of RIKEN (to T. K.), a RIKEN Presidential Research Grant for Intersystem Collaboration (to T. K. and A. Y.-H.), and Grants-in-aid 12672143 and 14370753 (to T. K.), 12680616 and 14021114 (to K. Iwabuchi), and 13771400 (to A. Y.-H.) from the Ministry of Education, Culture, Sports, Science, and Technology of Japan. The costs of publication of this article were defrayed in part by the payment of page charges. This article must therefore be hereby marked "*advertisement*" in accordance with 18 U.S.C. Section 1734 solely to indicate this fact.

¶ To whom correspondence may be addressed: RIKEN, 2-1, Hirosawa, Wako, Saitama 351-0198, Japan. Tel.: 81-48-467-9612; Fax: 81-48-467-8693; E-mail: sbsato@em.biophys.kyoto-u.ac.jp.

** A special postdoctoral fellow of RIKEN.

¶¶ Supported by Ara Parseghian Medical Research Foundation, Ono Medical Research Foundation, and International HDL Award Program. To whom correspondence may be addressed: RIKEN, 2-1, Hirosawa, Wako, Saitama 351-0198, Japan. Tel.: 81-48-467-9612; Fax: 81-48-467-8693; E-mail: kobayasi@riken.jp.

[1] The abbreviations used are: MβCD, methyl-β-cyclodextrin; Chol, cholesterol; PEG-Chol, poly (ethylene glycol)-derivatized cholesterol; fPEG-Chol, fluorescein ester of poly (ethylene glycol)-derivatized cholesterol; CTxB, cholera toxin B subunit; DOPC, dioleoylphosphatidylcholine; DHE, dehydroergosterol; GlcCer, glucosylceramide; GM1, Galβ1,3GalNAcβ1,4(NeuAcα2,3)Galβ1,4GlcCer; NPC, Niemann-Pick type C; POPC, palmitoyloleoylphosphatidylcholine; SM, sphingomyelin; TRITC, tetramethylrhodamine isothiocyanate; CHO, Chinese hamster ovary; EGF, epidermal growth factor; TGN, trans-Golgi network.

PEG-Chol (fPEG-Chol) partitioned from an aqueous media into cholesterol-rich membranes both in cells and in model membranes. These properties of fPEG-Chol made it possible to apply this compound to follow the re-organization of cell surface cholesterol as well as intracellular cholesterol dynamics. Moreover, because fPEG-Chol is water soluble and does not transverse lipid bilayer, we could localize cholesterol-rich domains in the cytoplasmic leaflet of intracellular organelle by microinjection.

MATERIALS AND METHODS

Cells and Reagents—Cultured skin fibroblasts from patients with Niemann-Pick type C (NPC) and from healthy subjects were established and maintained as described (12). Mouse melanoma cell line MEB4 and its glycosphingolipid-deficient mutant GM95 (13) were generous gifts of Dr. Yoshio Hirabayashi (Brain Science Institute, RIKEN). The cells were cultured in Dulbecco's modified Eagle's medium supplemented with 10% fetal calf serum, 100 units/ml penicillin, and 100 μg/ml streptomycin. COS7 cells were gown in RPMI 1640 medium containing 10% fetal calf serum, 100 units/ml penicillin, and 100 μg/ml streptomycin. Chinese hamster ovary (CHO) cells were grown as described (14). Cholesterol was purchased from Sigma. 2-(4,4-Difluoro-5,7-dimethyl-4-bora-3a,4a-diaza-*s*-indacene-3-dodecanoyl)-1-hexadecanoyl-*sn*-glycero-3-phosphocholine (BODIPY-C12-PC), Alexa Fluor 546-labeled cholera toxin B subunit (CTxB), Alexa Fluor 594-labeled CTxB, Texas Red transferrin, and rhodamine dextran were purchased from Molecular Probes (Eugene, OR). All other lipids were from Avanti polar lipids (Alabaster, AL). Anti-TGN46 antibody was from Serotec (Oxford, UK). Phycoerythrin-conjugated anti-CD59 monoclonal antibody was purchased from Pharmingen (San Diego, CA). Randomly methylated-β-cyclodextrin was from Cyclolab (Budapest, Hungary).

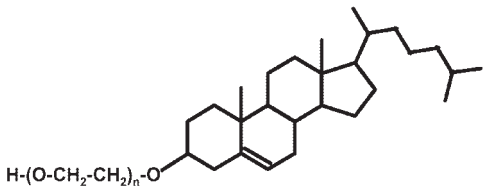

FIG. 1. **Structure of PEG-Chol.**

Binding of fPEG-Chol to Cholesterol-containing Liposomes—1 mM sphingomyelin (SM) vesicles containing various amount of cholesterol were analyzed the binding of fPEG-Chol. Vesicles were prepared as described (15) and incubated with 2 μM fPEG-Chol for 30 min at room temperature. Unbound fPEG-Chol was washed with centrifugation at 15,000 $\times$ *g* for 15 min. Fluorescence of the pellet was measured and normalized by phosphorous of SM.

Transfer of fPEG-Chol between Membranes—250 μM (final concentration of phospholipids) acceptor liposomes were added to 50 μM donor palmitoyloleoylphosphatidylcholine (POPC) liposomes containing 0.5 μM fPEG-Chol and 0.5 μM *N*-rhodamine dipalmitoylphosphatidylethanolamine. The release of fluorescence resonance energy transfer was measured at 30 °C by monitoring the time course of fluorescence emission spectrum at 535 nm with excitation at 488 nm.

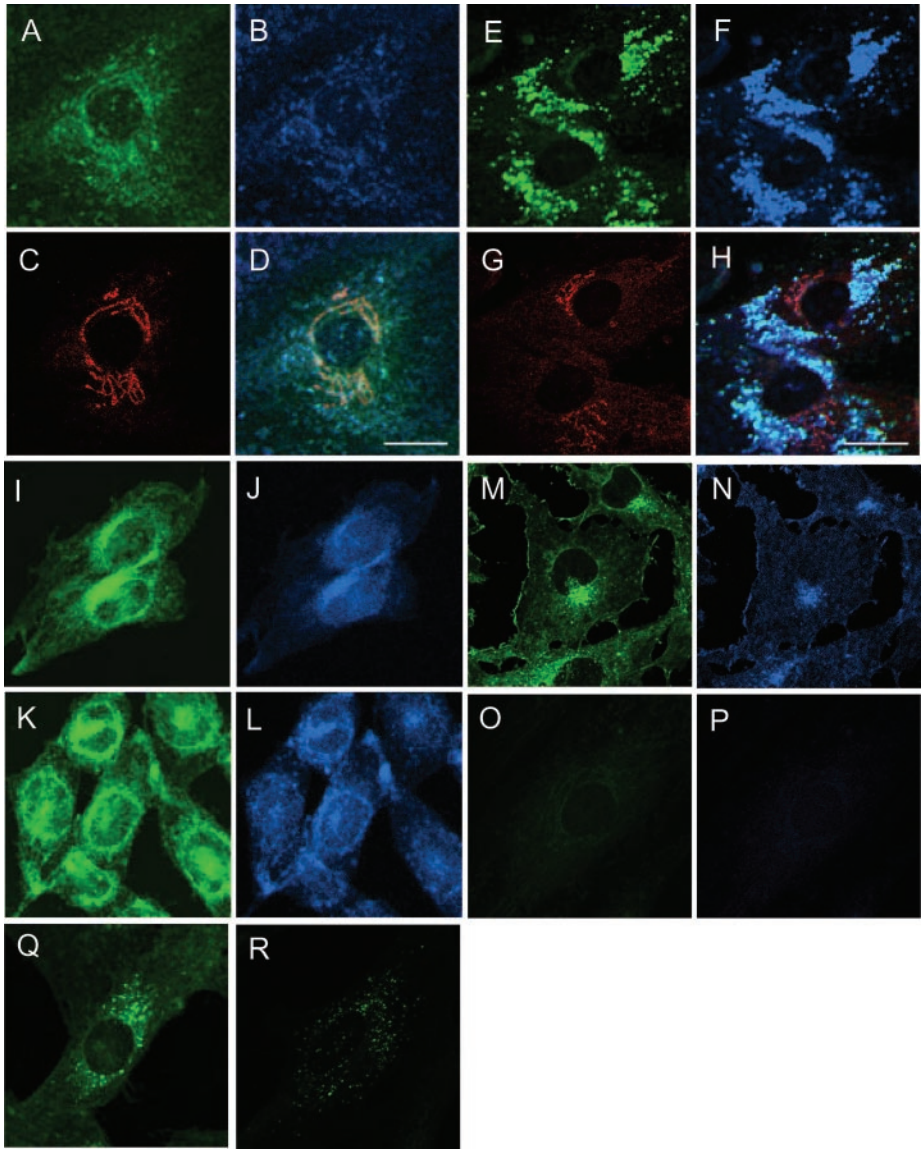

FIG. 2. **PEG-Chol stains cholesterol-rich membrane domains.** Normal (*A–D*) and NPC (*E–H*) human skin fibroblasts were fixed and permeabilized as described under "Materials and Methods." Cells were then triply labeled with 5 μM fPEG-Chol (*A* and *E*), 50 μg/ml filipin (*B* and *F*), and anti-TGN46 antibody (*C* and *G*). *D* and *H* show merged images. *White color* indicates the co-localization of three fluorophores. For fPEG-Chol- and filipin-stained samples, normal cells and NPC cells were exposed differently to acquire images since the fluorescence is much brighter in NPC cells. Mouse melanoma MEB4 (*I* and *J*), its derivative with defective in glycolipid synthesis, GM95 (*K* and *L*), and COS7 cells (*M* and *N*) were doubly labeled with fPEG-Chol (*I*, *K*, and *M*) and filipin (*J*, *L*, and *N*). *O* and *P*, fixed and permeabilized NPC cells were treated with 10 mM MβCD for 30 min at 37 °C. Cells were then doubly labeled with PEG-Chol (*O*) and filipin (*P*) as described above. *Q* and *R*, NPC skin fibroblasts were fixed and permeabilized. Cells were then labeled with 5 μM fPEG-Chol in the presence of 1 mM SM liposomes (*Q*) or SM/cholesterol (1:1) liposomes (*R*). *Bar*, 20 μm.

Loading Dehydroergosterol (DHE) on MβCD—DHE·MβCD complex was prepared as described (16). In brief, DHE in ethanol was dried under argon and subsequently dissolved in MβCD in Medium 1 (150 mM NaCl, 5 mM KCl, 1 mM $CaCl_2$, 1 mM $MgCl_2$, and 20 mM Hepes, pH 7.4), making the initial ratio of MβCD to DHE 8:1 (mol:mol). The resulting suspension was vortexed and sonicated until it clarified. It was then incubated in a rocking water bath overnight at 37 °C and centrifuged to remove insoluble DHE aggregates.

Microscopy—For immunofluorescence of fixed and permeabilized fibroblasts, cells were incubated with 3% paraformaldehyde followed by the treatment with 50 μg/ml digitonin for 5 min at room temperature before the addition of the antibody. The specimens were observed using Zeiss LSM 510 confocal microscope. In Fig. 4, the specimens were observed under an Olympus BX50 microscope equipped with a Hamamatsu C-4742-98 cooled CCD camera, which was controlled by a MetaView imaging software. In Fig. 6, fluorescence microscopy and digital image acquisition were carried out using an Olympus IX71 microscope equipped with UPlan Apo 100× objective. Images were acquired using a Hamamatsu Image Intensifier Unit C8600 connected with a C-2400 CCD camera. DHE was imaged using a filter cube obtained from Chroma Technology Corp. (Brattleboro, VT) (335-nm (20-nm bandpass) excitation filter, 365-nm longpass dichromatic filter, and 405-nm (40 nm bandpass) emission filter).

RESULTS

PEG-Chol and Filipin Similarly Localized Cholesterol-rich Membranes in Fixed and Permeabilized Cells—We prepared a fluorescein ester of PEG-Chol that contains a fluorescein on the distal end of PEG chain (fPEG-Chol, (9)). fPEG-Chol was added to fixed and digitonin-permeabilized normal human skin fibroblasts (Fig. 2, *A–D*). After washing by a conventional immunofluorescence protocol, the Golgi apparatus and intracellular small vesicles became fluorescent (Fig. 2*A*). The pattern of fPEG-Chol fluorescence was very similar to that of filipin (Fig. 2*B*). As described previously (17), we defined partial colocalization of fPEG-Chol and the immunofluorescence for a trans-Golgi network (TGN) marker, TGN46, in the Golgi (Fig. 2, *C* and *D*) (18). NPC is an autosomal recessive, neurovisceral disease. The hallmark of the NPC syndrome is the intracellular accumulation of unesterified cholesterol (12, 19, 20). In contrast to normal fibroblasts, fPEG-Chol brightly stained numerous perinuclear compartments that were previously identified as lysobisphosphatidic acid-rich late endosomes (12). In contrast, the appearance of the Golgi apparatus was normal in the NPC cells (Fig. 2*G*). Again, the fluorescence was co-localized with filipin fluorescence (Fig. 2, *E* and *F*). Co-localization of fPEG-Chol and filipin were observed in other cell types such as melanoma cells (Fig. 2, *I* and *J*), and their derivatives, which are deficient in glycolipid synthesis (Fig. 2, *K* and *L*) (13) as well as COS7 cells (Fig. 2, *M* and *N*). Both fPEG-Chol and filipin staining were abolished when cells were pretreated with MβCD (Fig. 2, *O* and *P*), which removes cholesterol from cells (21). fPEG-Chol labeling was reduced when fPEG-Chol was preincubated with SM/Chol (1:1) liposomes (Fig. 2*R*). A similar result was obtained with PC/Chol (1:1) liposomes. Chol-free SM or PC liposomes were much less effective to decrease fPEG-Chol labeling (Fig. 2*Q*).

PEG-Chol Is Preferentially Distributed to Cholesterol-rich Membranes in Model Membranes—The results in fixed-permeabilized cells suggested the preference of fPEG-Chol to cholesterol-containing membranes. When SM liposomes were mixed with fPEG-Chol, the addition of cholesterol increased the fluorescence recovered with the membrane (Fig. 3*A*). In Fig. 3, *B* and *C*, we incubated fPEG-Chol pre-embedded in POPC liposomes with various liposomes. The fluorescence of fPEG-Chol was initially quenched by including an acceptor molecule of fluorescence resonance energy transfer, *N*-rhodamine phosphatidylethanolamine (22, 23). These liposomes were mixed with acceptor liposomes that contained no probe. Because rhodamine phosphatidylethanolamine is a non-exchangeable

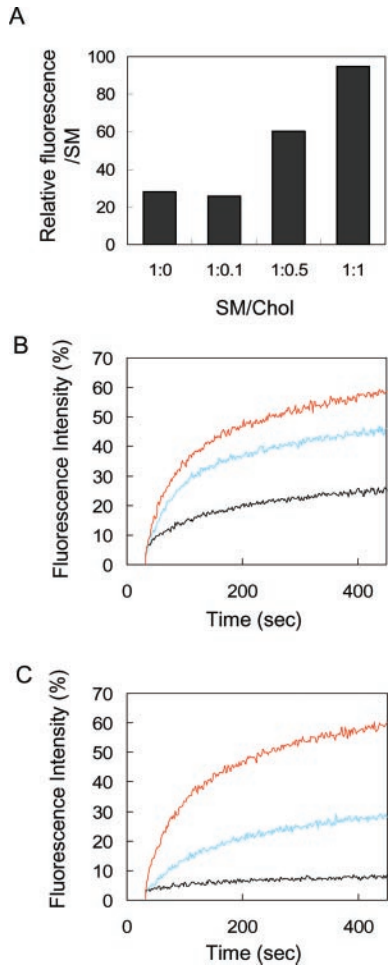

FIG. 3. **PEG-Chol preferentially distributes to cholesterol-rich membranes.** *A*, 1 mM SM vesicles containing various amount of cholesterol was analyzed the binding of fPEG-Chol. Vesicles were prepared as described (15). Vesicles were incubated with fPEG-Chol for 30 min at room temperature. Unbound fPEG-Chol was washed with centrifugation at 15,000 × *g* for 15 min. Fluorescence of the pellet was measured and normalized by phosphorous of sphingomyelin. PEG-Chol preferentially partitions to cholesterol-rich membranes. Relative fluorescence/sphingomyelin at different sphingomyelin/cholesterol molar ratios is indicated. *B* and *C*, 50 μM POPC donor liposomes containing 0.5 μM fPEG-Chol and 0.5 μM *N*-rhodamine-dipalmitoylphosphatidylethanolamine were incubated with 250 μM (final concentration of POPC) (*black*), POPC/Chol (1:1) (*blue*), and POPC/Chol (1:2) (*red*) (*B*) or 250 μM (final concentration of SM) SM (*black*), SM/Chol (1:1) (*blue*), and SM/Chol (1:2) (*red*) (*C*) acceptor liposomes. Transfer was measured as described under "Materials and Methods."

phospholipid, once fPEG-Chol moved into the acceptor liposomes, its fluorescence would be de-quenched. Remarkably, fluorescence was dequenched depending on the cholesterol content of liposomes. In contrast, cholesterol-containing liposomes did not release the quenching of non-exchangeable *N*-NBD-phosphatidylethanolamine fluorescence in rhodamine-phosphatidylethanolamine/phosphatidylcholine/PEG-Chol liposomes (data not shown). These results indicated that fPEG-Chol moved from phosphatidylcholine liposomes to cholesterol-containing liposomes via aqueous transfer but not by membrane fusion. Our results suggest that, even once embedded in cholesterol-free membranes, fPEG-Chol will move to cholesterol-rich membranes.

PEG-Chol Reveals Re-organization of Cell Surface Cholesterol-rich Domains—Unlike filipin and DHE, fPEG-Chol is membrane non-permeable (see below). This characteristic made it possible to examine the detailed distribution of cell surface cholesterol by fPEG-Chol. In Fig. 4 we examined the distribu-

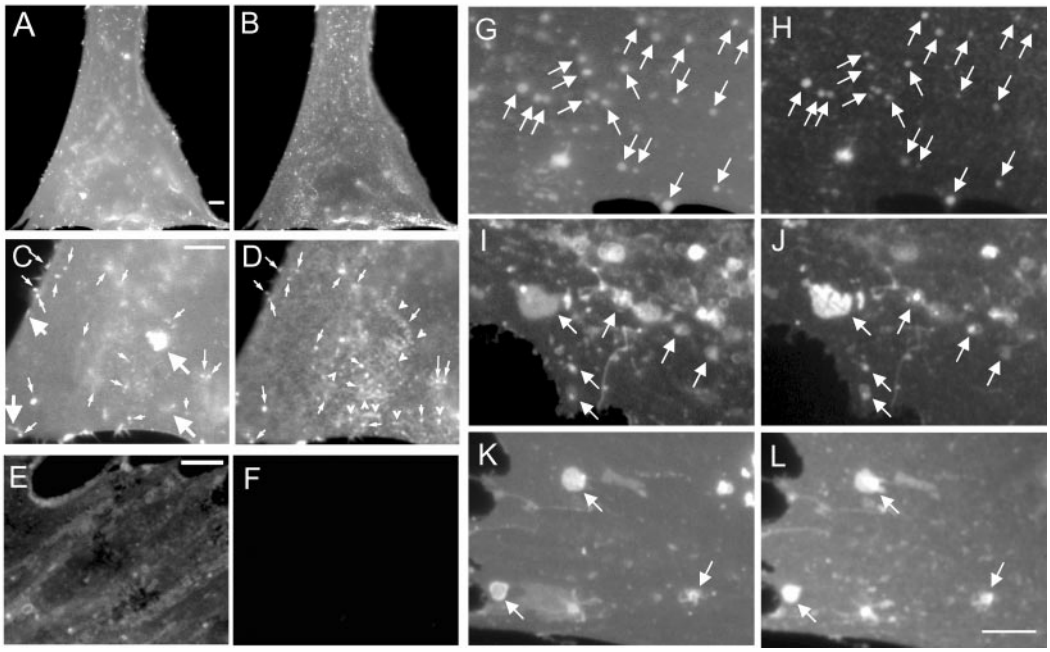

FIG. 4. **PEG-Chol reveals re-distribution of cholesterol-rich plasma membrane domains in fibroblasts.** *A–D*, normal human skin fibroblasts were incubated with 1 μM fPEG-Chol and 5 μM AlexaFluor 594-labeled cholera toxin for 90 s at room temperature and then fixed with paraformaldehyde for 10 min. *A* and *C*, fPEG-Chol fluorescence. *B* and *D*, AlexaFluor 594 fluorescence. *Small arrows* show the structures that were doubly labeled with fPEG-Chol and cholera toxin. *Big arrows* show those labeled solely with fPEG-Chol. *Arrowheads* indicate the spots positive with cholera toxin alone. In *E* and *F*, cells were treated with (*F*) and without (*E*) 10 mM MβCD for 30 min at 37 °C before fixation. Cells were then labeled with 1 μM fPEG-Chol. *Bar*, 4 μm. *G–L*, normal skin fibroblasts were labeled with 2 μM fPEG-Chol and incubated with 5 μg/ml biotinylated EGF for 20 min at 4 °C (*G* and *H*) or for 2 min at 37 °C (*I–L*). Cells were then fixed with 3% paraformaldehyde, 8% sucrose in phosphate-buffered saline, quenched, and incubated with TRITC-labeled streptavidin for 20 min at 4 °C. The specimens were observed under Nikon TE 300 microscope equipped with Hamamatsu C-4742–98 cooled CCD camera. *G* and *I*, fPEG-Chol fluorescence. *H* and *J*, TRITC-fluorescence. In *K* and *L*, cells were doubly labeled with 1 μM fPEG-Chol- and AlexaFluor 594-labeled cholera toxin B subunit before stimulation by non-labeled EGF. *K*, fPEG-Chol fluorescence. *L*, cholera toxin fluorescence. *Arrows* show the structures that were doubly labeled. *Bar*, 4 μm.

tion of fPEG-Chol on the cell surface by wide-angle video-enhanced microscopy. After a brief incubation with fPEG-Chol and subsequent wash and fixation (the whole procedure was completed within 2 min), we could detect uneven distribution of fluorescence (Fig. 4, *A* and *C*). Many of fPEG-positive area were co-localized with CTxB (Fig. 4, *B* and *D*). CTxB binds to GM1, which is non-randomly distributed on the plasma membranes, and accumulates in rafts/caveolae (24). This surface staining was abolished when cells were treated with MβCD (Fig. 4, *E* and *F*). We also measured the distribution of fPEG-Chol in cells shortly after the stimulation with epidermal growth factor (EGF). It is suggested that EGF receptor localizes cholesterol-rich plasma membrane domains and that binding of EGF to the receptor is dependent on cell surface cholesterol (25–27). fPEG-Chol fluorescence was co-localized with the distribution of biotin-labeled EGF when EGF was added at 4 °C (Fig. 4, *G* and *H*). When EGF was added at 37 °C, clustering of the EGF receptors was observed (Fig. 4*J*). These clusters were labeled with fPEG-Chol (Fig. 4*I*). The cell surface distribution of GM1 was also examined under these conditions. GM1 was also enriched in these clusters and co-localized with fPEG-Chol (Fig. 4, *K* and *L*). These results indicate that EGF induced the re-distribution of both fPEG-Chol and GM1 to the same clusters where EGF receptors were enriched.

fPEG-Chol in the Outer Plasma Membrane Leaflet Is Slowly Internalized Together with Lipid Raft Markers—Previously it was shown that PEG-Chol specifically inhibits clathrin-independent endocytosis (9, 11). Endocytosis was significantly reduced when cells were preincubated with 2.5 μM or higher concentrations of PEG-Chol for 30 min at 37 °C. When human skin fibroblasts were incubated with 2.5 μM PEG-Chol for 30 min at 37 °C, cells internalize 37 ± 8 pmol of PEG-Chol/mg of protein. Endocytosis was not affected when cells were briefly incubated with low concentrations of PEG-Chol. Therefore, it is possible to follow the fate of cell surface PEG-Chol in living cells under these conditions. We treated cells with 1 μM fPEG-Chol for 5 min at room temperature. Under these conditions cells incorporated 1.8 ± 0.3 pmol of fPEG-Chol/mg of protein. This amount of fPEG-Chol was sufficient to follow the fate of fluorescence. However, this concentration of fPEG-Chol did not affect the endocytosis of dextran and CTxB. After labeling cells with fPEG-Chol, we chased the internalization of fluorescence at 37 °C in the presence of 1 mg/ml rhodamine dextran. Most of the fPEG-Chol fluorescence stayed on the plasma membrane after 10 min of chase (Fig. 5, *A* and *D*). After 60 min, fluorescent compartments surrounded the nucleus (Fig. 5*B*). fPEG-Chol could further stain intracellular vesicles. Most of these vesicles were not co-localized with internalized rhodamine dextran (Fig. 5*E*). After 180 min, the Golgi apparatus was prominently labeled with fPEG-Chol whereas rhodamine fluorescence was distributed in endosomes/lysosomes (Fig. 5, *C* and *F*). fPEG-Chol fluorescence in intracellular vesicles was highly enhanced after neutralizing the vesicular pH by ammonium chloride (Fig. 5, *G* and *H*). We then compared the internalization of fPEG-Chol with those of known raft markers. Cells were preincubated with the PE-conjugated monoclonal antibody against glycosylphosphatidylinositol-anchored protein, CD59 (Fig. 5, *L–N*), Alexa-594 labeled CTxB (Fig. 5, *O–Q*) or Texas Red-labeled transferrin (Fig. 5, *I–K*) together with fPEG-Chol. After washing, cells were incubated for 20 min at 37 °C, treated with ammonium chloride at room temperature, and then immediately observed. fPEG-Chol well co-localized with lipid raft markers CD59 and GM1. In contrast, fPEG-Chol was not co-localized with internalized transferrin. Transferrin is internalized via clathrin-dependent endocytosis, whereas glycosylphosphatidylinositol-anchored proteins and cholera toxin are

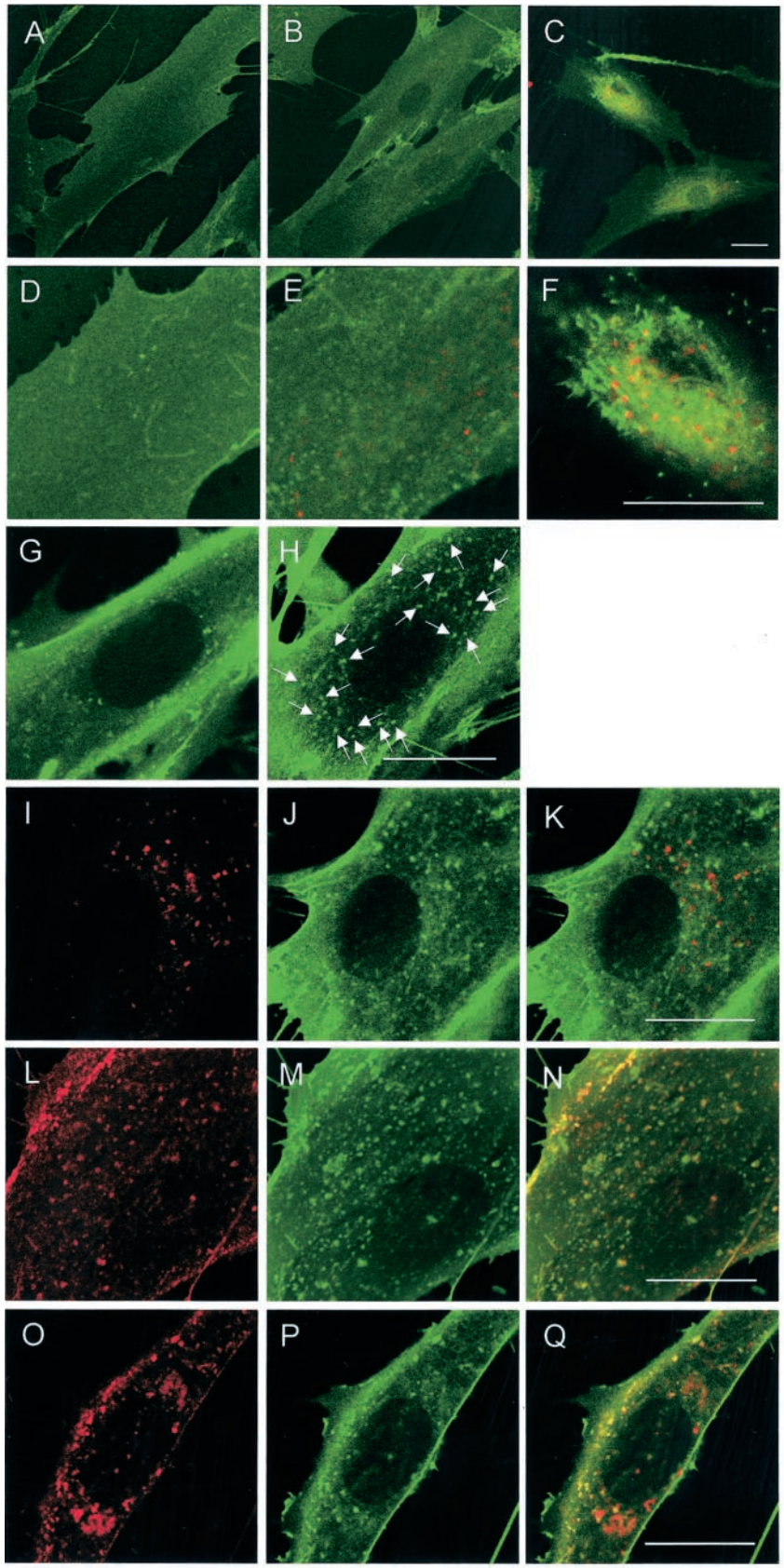

FIG. 5. **PEG-Chol is internalized together with lipid raft components.** *A–F*, normal human skin fibroblasts were incubated with 1 μM fPEG-Chol for 5 min at room temperature. Cells were then washed and incubated for 10 (*A* and *D*), 60 (*B* and *E*), and 180 min (*C* and *F*) at 37 °C in the presence of 1 mg/ml rhodamine dextran. *G* and *H*, normal fibroblasts were incubated with 1 μM fPEG-Chol for 5 min at room temperature. Cells were washed and incubated at 37 °C for 20 min. Cells were then photographed (*G*) or treated with 10 mM ammonium chloride before imaging (*H*). *Arrows* show vesicle like structures. *I–Q*, normal fibroblasts were incubated with 1 μM fPEG-Chol together with Texas Red transferrin (*I–K*), AlexaFluor 594-labeled CTxB (*L–N*), or phycoerythrin-conjugated anti-CD59 monoclonal antibody (*O–Q*) for 5 min at room temperature. Cells were then washed and further incubated for 20 min. Cells were treated with ammonium chloride before taking images. *Bar*, 20 μm.

endocytosed by clathrin-independent mechanisms (28). Our results suggest that the raft domains were internalized via clathrin-independent pathway into acidic organelle. During prolonged incubation, fPEG-Chol was further transported to the Golgi apparatus.

Recently intracellular transport of cell surface cholesterol in CHO cells was studied by using DHE (16). DHE was enriched in the endocytic recycling compartment. We then compared the internalization of fPEG-Chol with that of DHE in CHO cells. As reported, DHE was detected in the juxta-nuclear region (Fig.

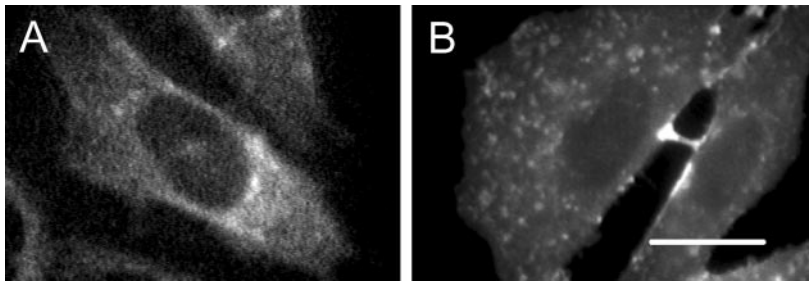

FIG. 6. **fPEG-Chol and DHE are differently internalized.** *A*, CHO cells were pulsed with DHE-loaded MβCD for 5 min at 37 °C and chased for 90 min in Medium 1 (150 mM NaCl, 5 mM KCl, 1 mM $CaCl_2$, 1 mM $MgCl_2$, and 20 mM Hepes, pH 7.4) containing 2 g/liter glucose (M1 glucose). *B*, CHO cells were labeled with 1 μM fPEG-Chol for 5 min at room temperature. Cells were then washed and incubated in M1 glucose for 90 min. Cells were treated with ammonium chloride before imaging. For both panels cells were imaged at room temperature. Cells were not doubly labeled with DHE and fPEG-Chol because fPEG-Chol binds DHE. *Bar*, 20 μm.

6*A*). In contrast, fPEG-Chol fluorescence was seen in intracellular vesicles (Fig. 6*B*). These results indicate that the intracellular fates of fPEG-Chol and DHE are different.

Cytoplasmic Leaflet of the Golgi Apparatus Has Cholesterol-rich Domains—In Fig. 7*A*, living human skin fibroblasts were labeled with fPEG-Chol at 10 °C, a condition that inhibits endocytosis. Fluorescence shows exclusive cell surface staining. This pattern of distribution was remarkably different from that of a fluorescent phosphatidylserine derivative, 1-palmitoyl-2-(6-((7-nitro-2-1,3-benzoxadiazol-4-yl)amino)hexanoyl)-*sn*-glycero-3-phospho-L-serine (C6-NBD-phosphatidylserine), which has been known to be incorporated into the plasma membrane and to undergo transbilayer movement and intracellular diffusion (29, 30). In Fig. 7*B*, C6-NBD-phosphatidylserine was accumulated in the Golgi apparatus and mitochondria after 30 min at 10 °C, in agreement with previous observations (30). These results indicate that fPEG-Chol does not undergo transbilayer movement and is membrane-impermeable.

Little is known about the transbilayer membrane distribution of cholesterol in live cell organelles. Because fPEG-Chol is membrane-impermeable, we microinjected this molecule in live cells to monitor the distribution of cholesterol in the cytoplasmic side of intracellular organelles. When we microinjected fPEG-Chol in living normal skin fibroblasts, fluorescence illuminated the Golgi apparatus (Fig. 7*C*). Surprisingly, the pattern was similar in NPC cells. The numerous cholesterol-rich late endosomes, which could be detected in fixed and permeabilized cells (Fig. 2*E*), were not labeled at all (Fig. 7*D*). These results suggest that the Golgi apparatus solely exposes cholesterol-rich domains to the cytoplasm of both the normal and NPC fibroblasts. Microinjection of fPEG-Chol did not inhibit the endocytosis of rhodamine dextran. After prolonged incubation, fluorescence was dispersed throughout the cytoplasm (data not shown).

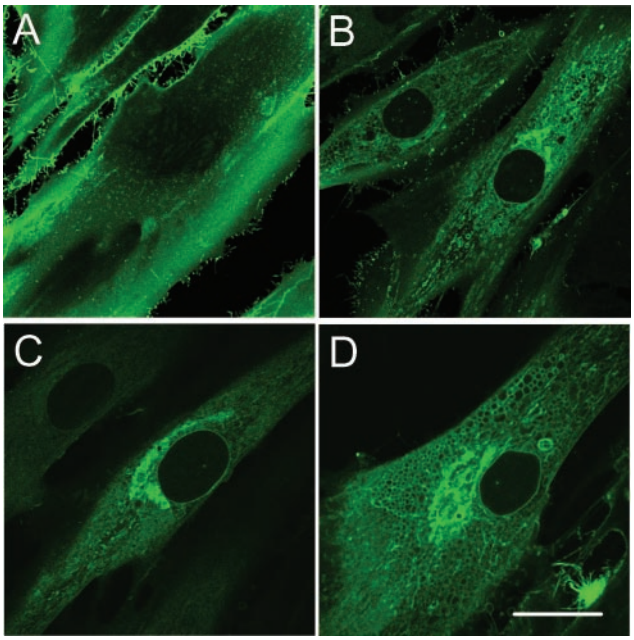

FIG. 7. **Microinjected fPEG-Chol is accumulated in the Golgi apparatus.** Human skin fibroblasts were incubated with 1 μM fPEG-Chol (*A*) or 1 μM C6-NBD-phosphatidylserine (*B*) for 30 min at 10 °C. Cells were washed, and fluorescence images were immediately recorded under confocal microscope. *C* and *D*, 100 μM fPEG-Chol in 25 mM Hepes-KOH, pH 7.0, containing 25 mM KCl, 2.5 mM magnesium acetate, 0.25 M sucrose (23, 42) was microinjected to normal (*C*) and NPC (*D*) human skin fibroblasts at room temperature. Fluorescence images were observed under confocal microscope. *Bar*, 20 μm.

DISCUSSION

PEG-Chol, a Unique Water-soluble Probe for Cholesterol-rich Domains—Several probes have been used to localize cholesterol-rich domains. Filipin has spread widely (31) despite the limitation due to the high photosensitivity and toxicity (Ref. 32 and reference therein). Naturally occurring fluorescent cholesterol analog DHE has been used to follow the fate of unesterified sterol in living cells (16, 33)). Because DHE itself is water-insoluble and has a lower fluorescence quantum yield than conventional fluorophores, a substantial amount of this molecule has to be added to live cell studies in a form complexed with MβCD. These conditions may become an obstacle in some experiments since chronic treatment of cells with MβCD-cholesterol alters cellular lipid metabolism (34). Recently a novel protein probe (BCθ) derived from bacterial toxin, perfringolysin O, has been shown to selectively bind to cholesterol-rich membrane domains (32, 35–37). However, because BCθ is a bulky protein (M_r ~ 57 kDa), it may induce an alteration of the membrane organization.

Although liposome studies suggested that fPEG-Chol has background distribution into the hydrophobic membrane milieu as other hydrophobic molecules do, it showed the following unique characteristics: 1) preferential partition to cholesterol-rich membranes such as SM/Chol, 2) higher stability and quantum efficiency of the fluorophore than DHE or filipin, 3) single dispersion in aqueous phase at ~μM concentrations, 4) low cell toxicity, 5) unlikely to permeate or flip-flop membranes, 6) relatively low molecular weight (~2,600). We stress that these properties of fPEG-Chol not only complemented the information obtained by other probes but also uncovered the yet unknown trafficking of cholesterol-containing membranes in live cells.

Cellular Distribution of Cholesterol-rich Domains—An *in vitro* study indicates that fPEG-Chol is useful in documenting

dynamics of raft-like structures inside the cells as well as on the surface. Although the presumably high mobility on the surface may not allow complete visualization in the living cells, short exposure to fPEG-Chol revealed numerous spots on the cell surface. This probe followed the reorganization of these domains after activation of EGF signaling, in which fPEG-Chol aggregated with EGF and GM1.

With fPEG-Chol, late endosomes were stained in fixed normal and Niemann-Pick type C cells. Interestingly, even in NPC fibroblasts, microinjection of fPEG-Chol illuminated for the first time the Golgi apparatus, but not late endosomes, as the sole major organelle that exposes cholesterol-rich domain cytoplasmically. Late endosomes were previously shown to be highly enriched with a specific phospholipid, lysobisphosphatidic acid (12, 38–40). Luminal binding of several antibodies to this lipid interferes with its function in accumulation and distribution of cholesterol. Our present results suggest that accumulated cholesterol and lysobisphosphatidic acid reside in the same luminal leaflet, raising the possibility of direct interaction between these molecules in NPC.

Fate of Cell Surface Cholesterol—Recently intracellular transport of cell surface cholesterol in CHO cells was studied by using a DHE/MβCD (16). DHE was enriched in the endocytic recycling compartment localized by transferrin. The delivery of DHE to the endocytic recycling compartment from the plasma membrane was only slightly affected by energy depletion, suggesting the involvement of a non-vesicular pathway. Our results indicate that the routes of internalization of DHE and PEG-Chol are different. Because DHE undergoes rapid transbilayer movement (41), such a mechanism may involve spontaneous flip-flop of the molecule from the outer to inner plasma membrane leaflets followed by the accumulation to an endocytic recycling compartment (16). In contrast, fPEG-Chol restricted in the outer leaflet cholesterol-rich domain likely monitored the slow clathrin-independent traffic to the Golgi region. We suggest here that the trafficking of the cholesterol in the outer and inner plasma membrane monolayers occur independently.

REFERENCES

1. Bretscher, M. S., and Munro, S. (1993) *Science* **261,** 1280–1281
2. Brown, D. A., and London, E. (1998) *Annu. Rev. Cell Dev. Biol.* **14,** 111–136
3. Kurzchalia, T. V., and Parton, R. G. (1999) *Curr. Opin. Cell Biol.* **11,** 424–431
4. Simons, K., and Toomre, D. (2000) *Nat. Rev. Mol. Cell. Biol.* **1,** 31–39
5. Maxfield, F. R. (2002) *Curr. Opin. Cell Biol.* **14,** 483–487
6. Pike, L. J., and Miller, J. M. (1998) *J. Biol. Chem.* **273,** 22298–22304
7. Roper, K., Corbeil, D., and Huttner, W. B. (2000) *Nat. Cell Biol.* **2,** 582–592
8. Kuwabara, P. E., and Labouesse, M. (2002) *Trends Genet* **18,** 193–201
9. Ishiwata, H., Sato, S. B., Vertut-Doi, A., Hamashima, Y., and Miyajima, K. (1997) *Biochim. Biophys. Acta* **1359,** 123–135
10. Tasset, C., Preat, V., Bernard, A., and Roland, M. (1992) *Antimicrob. Agents Chemother.* **36,** 1525–1531
11. Baba, T., Rauch, C., Xue, M., Terada, N., Fujii, Y., Ueda, H., Takayama, I., Ohno, S., Farge, E., and Sato, S. B. (2001) *Traffic* **2,** 501–512
12. Kobayashi, T., Beuchat, M. H., Lindsay, M., Frias, S., Palmiter, R. D., Sakuraba, H., Parton, R. G., and Gruenberg, J. (1999) *Nat. Cell Biol.* **1,** 113–118
13. Ichikawa, S., Nakajo, N., Sakiyama, H., and Hirabayashi, Y. (1994) *Proc. Natl. Acad. Sci. U. S. A.* **91,** 2703–2707
14. Endo, T. A., Kobayashi, T., and Ohki, K. (1996) *Exp. Cell Res.* **228,** 341–346
15. Miyazawa, A., Umeda, M., Horikoshi, T., Yanagisawa, K., Yoshioka, T., and Inoue, K. (1988) *Mol. Immunol.* **25,** 1025–1031
16. Hao, M., Lin, S. X., Karylowski, O. J., Wustner, D., McGraw, T. E., and Maxfield, F. R. (2002) *J. Biol. Chem.* **277,** 609–617
17. Orci, L., Montesano, R., Meda, P., Malaisse-Lagae, F., Brown, D., Perrelet, A., and Vassalli, P. (1981) *Proc. Natl. Acad. Sci. U. S. A.* **78,** 293–297
18. Prescott, A. R., Lucocq, J. M., James, J., Lister, J. M., and Ponnambalam, S. (1997) *Eur. J. Cell Biol.* **72,** 238–246
19. Pentchev, P. G., Brady, R. O., Blanchette-Mackie, E. J., Vanier, M. T., Carstea, E. D., Parker, C. C., Goldin, E., and Roff, C. F. (1994) *Biochim. Biophys. Acta* **1225,** 235–243
20. Liscum, L. (2000) *Traffic* **1,** 218–225
21. Rothblat, G. H., de la Llera-Moya, M., Atger, V., Kellner-Weibel, G., Williams, D. L., and Phillips, M. C. (1999) *J. Lipid Res.* **40,** 781–796
22. Nichols, J. W., and Pagano, R. E. (1982) *Biochemistry* **21,** 1720–1726
23. Kobayashi, T., and Pagano, R. E. (1988) *Cell* **55,** 797–805
24. Parton, R. G. (1994) *J. Histochem. Cytochem.* **42,** 155–166
25. Waugh, M. G., Minogue, S., Anderson, J. S., dos Santos, M., and Hsuan, J. J. (2001) *Biochem. Soc. Trans.* **29,** 509–511
26. Roepstorff, K., Thomsen, P., Sandvig, K., and van Deurs, B. (2002) *J. Biol. Chem.* **277,** 18954–18960
27. Ringerike, T., Blystad, F. D., Levy, F. O., Madshus, I. H., and Stang, E. (2002) *J. Cell Sci.* **115,** 1331–1340
28. Sabharanjak, S., Sharma, P., Parton, R. G., and Mayor, S. (2002) *Dev. Cell* **2,** 411–423
29. Martin, O. C., and Pagano, R. E. (1987) *J. Biol. Chem.* **262,** 5890–5898
30. Kobayashi, T., and Arakawa, Y. (1991) *J. Cell Biol.* **113,** 235–244
31. Norman, A. W., Demel, R. A., de Kruyff, B., and van Deenen, L. L. (1972) *J. Biol. Chem.* **247,** 1918–1929
32. Sugii, S., Reid, P. C., Ohgami, N., Shimada, Y., Maue, R. A., Ninomiya, H., Ohno-Iwashita, Y., and Chang, T. Y. (2003) *J. Lipid Res.* **44,** 1033–1041
33. Mukherjee, S., Zha, X., Tabas, I., and Maxfield, F. R. (1998) *Biophys. J.* **75,** 1915–1925
34. Blom, T. S., Koivusalo, M., Kuismanen, E., Kostiainen, R., Somerharju, P., and Ikonen, E. (2001) *Biochemistry* **40,** 14635–14644
35. Waheed, A. A., Shimada, Y., Heijnen, H. F., Nakamura, M., Inomata, M., Hayashi, M., Iwashita, S., Slot, J. W., and Ohno-Iwashita, Y. (2001) *Proc. Natl. Acad. Sci. U. S. A.* **98,** 4926–4931
36. Mobius, W., Ohno-Iwashita, Y., van Donselaar, E. G., Oorschot, V. M., Shimada, Y., Fujimoto, T., Heijnen, H. F., Geuze, H. J., and Slot, J. W. (2002) *J. Histochem. Cytochem.* **50,** 43–55
37. Mobius, W., Van Donselaar, E., Ohno-Iwashita, Y., Shimada, Y., Heijnen, H. F., Slot, J. W., and Geuze, H. J. (2003) *Traffic* **4,** 222–231
38. Kobayashi, T., Stang, E., Fang, K. S., de Moerloose, P., Parton, R. G., and Gruenberg, J. (1998) *Nature* **392,** 193–197
39. Kobayashi, T., Startchev, K., Whitney, A. J., and Gruenberg, J. (2001) *Biol. Chem.* **382,** 483–485
40. Kobayashi, T., Beuchat, M. H., Chevallier, J., Makino, A., Mayran, N., Escola, J. M., Lebrand, C., Cosson, P., and Gruenberg, J. (2002) *J. Biol. Chem.* **277,** 32157–32164
41. John, K., Kubelt, J., Muller, P., Wustner, D., and Herrmann, A. (2002) *Biophys. J.* **83,** 1525–1534
42. Balch, W. E., Dunphy, W. G., Braell, W. A., and Rothman, J. E. (1984) *Cell* **39,** 405–416